Letter

Ice Nucleation Properties of Oxidized Carbon Nanomaterials

Thomas F. Whale,*,† Martin Rosillo-Lopez,‡ Benjamin J. Murray,† and Christoph G. Salzmann‡

†Institute for Climate and Atmospheric Science, School of Earth and Environment, University of Leeds, Woodhouse Lane, Leeds LS2 9JT, United Kingdom

‡Department of Chemistry, University College London, 20 Gordon Street, London WC1H 0AJ, United Kingdom

S *Supporting Information*

ABSTRACT: Heterogeneous ice nucleation is an important process in many fields, particularly atmospheric science, but is still poorly understood. All known inorganic ice nucleating particles are relatively large in size and tend to be hydrophilic. Hence it is not obvious that carbon nanomaterials should nucleate ice. However, in this paper we show that four different readily water-dispersible carbon nanomaterials are capable of nucleating ice. The tested materials were carboxylated graphene nanoflakes, graphene oxide, oxidized single walled carbon nanotubes and oxidized multiwalled carbon nanotubes. The carboxylated graphene nanoflakes have a diameter of ~30 nm and are among the smallest entities observed so far to nucleate ice. Overall, carbon nanotubes were found to nucleate ice more efficiently than flat graphene species, and less oxidized materials nucleated ice more efficiently than more oxidized species. These well-defined carbon nanomaterials may pave the way to bridging the gap between experimental and computational studies of ice nucleation.
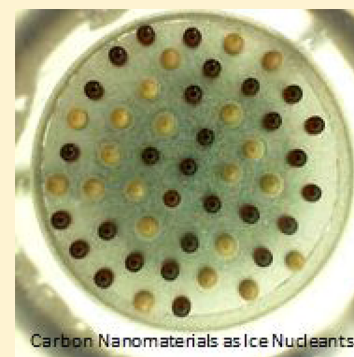
Carbon Nanomaterials as Ice Nucleants

Freezing of liquid water to ice must be initiated by an ice nucleation event. In many situations this event is induced by a heterogeneous ice nucleating particle (INP). Ice nucleation is an important process for understanding of atmospheric processes[1−3] and also has relevance in other fields such as the cryopreservation of biological samples,[4] freeze-drying of pharmaceuticals[5] and other substances,[6] and freezing of foodstuffs.[7] Much effort has been devoted to the quantification of the efficiencies of heterogeneous ice nucleants of potential atmospheric relevance. As such, the ice nucleating efficiencies of various mineral dusts, biological entities, volcanic ashes and carbonaceous combustion aerosols[8,9] have been measured using a wide range of techniques.[1,2]

It is often assumed that INPs tend to be relatively "large" in size.[3] Indeed, the concentration of atmospheric INPs is correlated with the concentration of particles larger than 0.5 μm in diameter.[10] However, it has been found that nanoscale, readily dispersible biological particles that are shed from both pollen particles and fungi in water can also nucleate ice efficiently,[11−13] and that small particles of poly(vinyl alcohol) can nucleate ice.[14] Of late, there has been a great deal of interest in the synthesis and characterization of carbon nanomaterials. Yet, the ice nucleation activities of these species have not been examined to date.

Here, we have synthesized four different carbon nanomaterials and determined their ice nucleating efficiencies. These are carboxylated graphene nanoflakes (cx-GNFs) and graphene oxide (GO) as well as oxidized multiwall (o-MWCNTs) and single-wall carbon nanotubes (o-SWCNTs). Representative structures for these species are shown in Figure 1. The oxygen/carbon ratios for these materials were determined by X-ray photoelectron spectroscopy (XPS). The cx-GNFs are small

graphene sheets with an average lateral diameter of ~30 nm.[15] The edges of the flakes are decorated with carboxylic acid groups. They contain 66.3% carbon and 33.7% oxygen. GO consists of much larger sheets of carbon, average diameter ~1 μm. The structure has a wider range of functional groups than that of the cx-GNFs with alcohol and epoxide groups present as well as carboxylic acids.[16] The face of the GO sheets is oxidized as well as the edges. The GO sample contains 72.0% carbon and 28.0% oxygen. MWCNTs are needle-like tubes of carbon and consist of multiple single layers of carbon wrapped concentrically. Our oxidized material contains 82.2% carbon and 17.8% oxygen. SWCNTs are structurally similar but consist of a single layer of carbon only. After chemical oxidation of the SWCNTs, we find 86.2% carbon and 13.8% oxygen according to XPS. We also present freezing data for a solution of mellitic acid, a molecular species structurally analogous to cx-GNFs, consisting of a single benzene ring with six carboxylic acid groups.

These materials were chosen for this study because their oxidized nature allows them to readily disperse in water. Attempts to conduct experiments with carbonized cx-GNFs, for example, proved impossible, as they did not disperse in water. The oxidized carbon nanomaterials, apart from the o-SWCNTs, all disperse readily in water with stirring. No more than 0.07 wt % of the o-SWCNTs could be dispersed. The 1 and 0.1 wt % dispersions of cx-GNFs are very stable and were not observed to settle even after several months. Suspensions of GO, o-MWCNTs, and o-SWCNTs were less stable, and settled over

(a) cx-GNF (b) mellitic acid
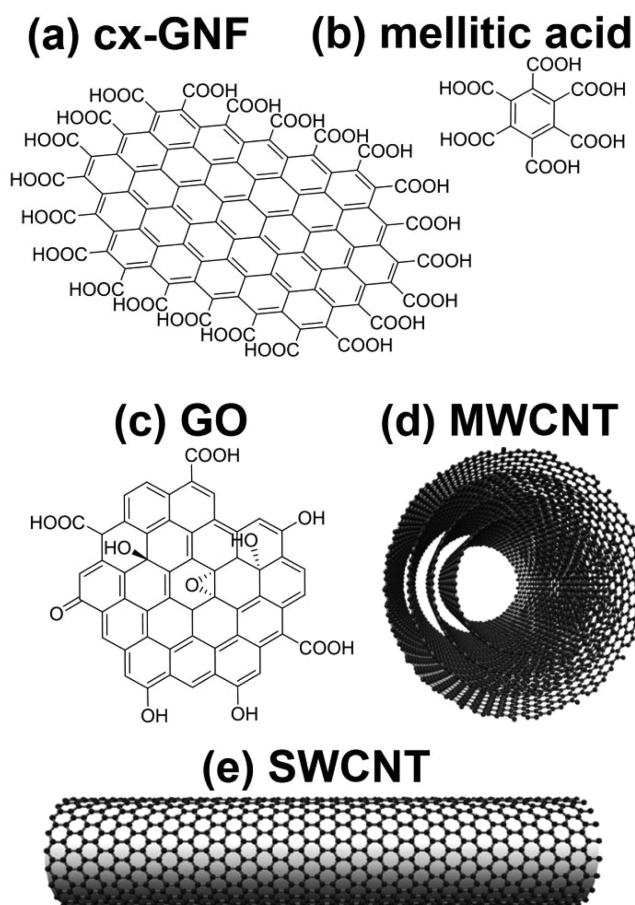
(c) GO (d) MWCNT

(e) SWCNT

Figure 1. Chemical structures of the various of carbon nanomaterials tested for their ice nucleation activity: (a) small carboxylated graphene nanoflake (cx-GNF), (b) mellitic acid, (c) graphene oxide (GO), (d) multiwalled carbon nanotube (MWCNT), and (e) single walled carbon nanotube (SWCNT). GO sheets have an average lateral diameter of ∼1 μm, while the GNFs have an average lateral diameter of ∼30 nm.[15]

◇ cx-GNFs 1 wt% △ GO 1 wt%
⬠ cx-GNFs 0.1 wt% ◯ GO 0.1 wt%
◁ o-MWCNTs 1 wt% □ Mellitic acid 1 wt%
▽ o-SWCNTs 0.07 wt% ── Pure water

Figure 2. (a) Droplet fraction frozen against temperature for 1 and 0.1 wt % dispersions of GO and cx-GNFs, a 1 wt % dispersion of o-MWCNTs, a 0.07 wt % dispersion of o-SWCNTs, a 1 wt % solution of mellitic acid, and pure water. (b) n_s values for all tested carbon nanomaterials. The n_s values reported for the o-MWCNTs assume that they have nine layers, the average number of the starting material for their synthesis. The shaded area shows the area encompassed by calculating n_s for the minimum and maximum wall numbers of the starting material. Experimental uncertainty in n_s was calculated by propagation of uncertainty from weighing, droplet size, and background subtraction. In many cases, uncertainties are too small to show on the plot. Temperature uncertainty is ±0.4 °C in panels a and b.

the course of hours. Dispersions of carbon nanomaterials were tested for the ice nucleating activity immediately after the preparation.

Ice nucleation experiments were conducted using the μL-Nucleation by Immersed Particles Instrument (μL-NIPI).[17] This instrument allows determination of the freezing temperatures of around 50 μL droplets of water under constant cooling. Here, a cooling rate of 1 °C min⁻¹ has been used. The freezing curve for pure water in Figure 2a consists of 737 separate freezing events from 17 experiments and has been reported previously by Umo et al.[18] The freezing observed in the pure water is unlikely to be induced by homogeneous nucleation, which is predicted by classical nucleation theory to occur at temperatures colder than −30 °C in 1 μL droplets.[19,20] Instead it is likely that the freezing observed is caused by a combination of impurities in the water and on the silanized glass slides used to support the droplets.

Droplets containing cx-GNFs, GO, o-MWCNTs, and o-SWCNTs all nucleate ice at temperatures higher than the pure water droplets, as shown in Figure 2a. This constitutes the first observations of ice nucleation by these types of materials. In contrast, it can be seen in Figure 2a that mellitic acid does not nucleate ice within the sensitivity of the experimental setup used, with recorded freezing temperatures indistinguishable to
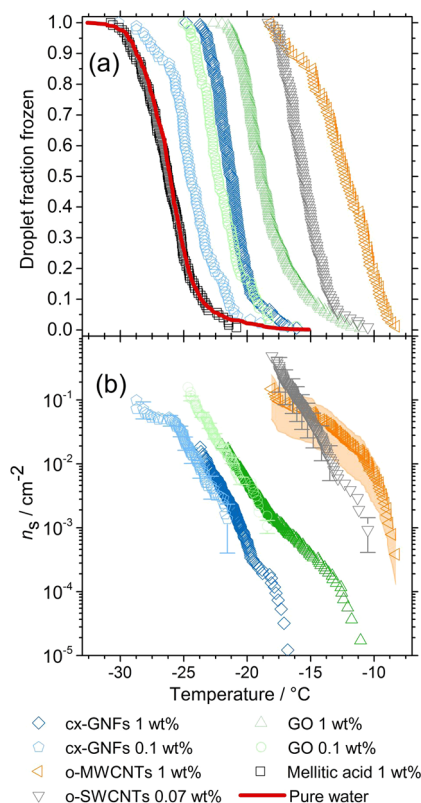
those of pure water. This is entirely expected as mellitic acid is a dissolved molecular species so there is no reason to suppose it would interact with water in a way that would encourage ice formation. It is interesting to note that the structurally analogous cx-GNFs do nucleate ice well, showing that the increase in size allows interactions with water suitable for encouraging ice nucleation to occur.

To allow comparison between the carbon nanomaterial nucleants, these values have been normalized to surface area according to a time-independent description of ice nucleation.[21,22] To calculate theoretical n_s values for the graphene species presented in Figure 2b, the total surface area of the cx-GNFs and GO was calculated by assuming that all graphene sheets were completely dissociated from each other and using

$$\frac{n(T)}{N} = 1 - \exp(-n_s(T)\sigma) \qquad (1)$$

where n_s is the cumulative number of surface sites per unit surface area of nucleant that become active on cooling from 273.15 K to a temperature T, σ is the surface area of nucleant per droplet, and $n(T)/N$ is the cumulative fraction of droplets frozen.

It can be seen in Figure 2a that GO nucleates ice more efficiently than the cx-GNFs per mass of material, and that the o-MWCNTs and o-SWCNTs nucleate ice more efficiently than the flat species. The carbon nanotubes (CNTs) are similar to each other. The shapes of the n_s curves for the two CNT species are different, however. The curve for the o-MWCNTs flattens at lower temperature, meaning that the number of effective INPs increases less quickly with increasing supersaturation than for the o-SWCNTs. There has been interest in the ordering of water in CNT cavities.[23] It is intriguing to suggest that the interior cavities of the CNTs interact with water in a way that promotes ice nucleation and that this is responsible for the strong nucleation we have observed. Both kinds of CNTs are rather less oxidized than the graphene species. The overall trend is therefore that the less oxidized species nucleate ice more efficiently. The 1 wt % dispersion of cx-GNFs has a median nucleation temperature of −21.3 °C and an oxygen content of 33.7%, while the 1 wt % dispersion of o-MWCNTs has a median nucleation temperature of −12.2 °C and an oxygen content of 17.8%. We note in this context that XPS is a surface-sensitive technique, and the determined atom percentages may therefore not necessarily reflect the bulk composition of the samples but more the composition of the sample at the interface with water.

The cx-GNFs in particular are light compared to most other INPs. Their average mass is approximately 325 kDa. In their recent paper, Pummer et al.[24] reviewed a range of small INPs. The cx-GNFs are comparable in mass to the Birch pollen-derived ice nucleating macromolecules discovered by Pummer et al.[11] and the fungal proteins sized by O'Sullivan et al.,[13] and somewhat larger than certain poly(vinyl alcohol)s discovered by Ogawa et al.,[14] which were shown to nucleate ice at molecular weights as low as 1.7 kDa. All other known INPs are heavier than the cx-GNFs.

The approach we have used to calculate n_s assumes that all possible surface area is in contact with water. It is hard to evaluate how realistic this is for the carbon nanomaterials, hence, the n_s values reported are most likely lower limits in the case of these nanomaterials. This also means that comparison with existing measurements of other carbon materials such as soots[8,9] is difficult. It can be seen in Figure 2b that n_s derived from lower concentrations dispersions of GO and cx-GNF fall on the same line as higher concentrations suggesting that similar surface areas of material are available per mass of material in both concentrations. This indicates that the materials are not aggregated in dispersion since aggregation is concentration dependent. Calculating n_s for the o-MWCNTs was less straightforward, as the precise number of layers in the MWCNTs from which the o-MWCNTs were synthesized is unknown. Manufacturer specifications for the starting material includes the maximum and minimum numbers of walls; n_s values have been calculated using these to provide upper and lower limits as seen in Figure 2b. We have assumed that the exterior surface area of the o-MWCNTs is solely responsible for nucleation observed and calculated surface area exposed to water on this basis. The interior surfaces may well play a role, even a dominant one, in the nucleation observed, but the assumptions made seem reasonable for comparative purposes.

While it is difficult to infer details about the specific mechanism of ice nucleation from droplet freezing experiments, some insight into the nature of ice nucleation observed can be derived from its time dependence. The Framework for Reconciling Observable Stochastic Time-dependence

(FROST) condenses the key information about time dependence of ice nucleation into a single parameter, λ, which is a nucleant-specific parameter that describes the time dependence of the ice nucleation properties (further details are given in the Supporting Information (SI)).[22] FROST facilitates comparison of different materials through calculation of λ using

$$T' = T - \frac{1}{\lambda}\left(\ln\frac{1}{r}\right) \tag{2}$$

where, for a given experiment, T' is the modified temperature, the freezing temperature that would be expected if an experiment were conducted at a standard rate of 1 °C min^{-1}, T is the measured freezing temperature, and r is the cooling rate in °C min^{-1}. To calculate λ from multiple fraction frozen curves, the difference between calculated T' values is minimized by varying λ iteratively.

We have cooled cx-GNFs at rates from 0.2 °C min^{-1} to 5 °C min^{-1}, the results of which are shown in Figure 3a, and
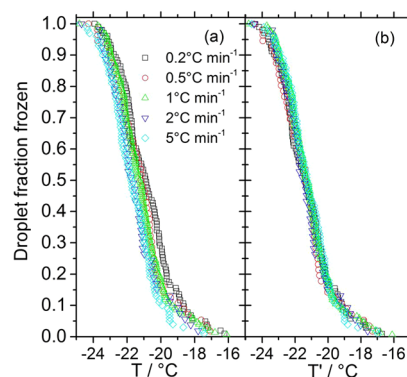

Figure 3. (a) Droplet fraction frozen against temperature for 1 wt % cx-GNFs at 5 different cooling rates. (b) Droplet fraction frozen against modified temperature as defined in eq 2 for the same experiments. Temperature uncertainty is ±0.4 °C in panels a and b.

analyzed the resulting data using FROST.[22] A λ value of 3.3 °C^{-1} has been determined, and Figure 3b shows the normalized data. This λ value is higher than those of the majority of nucleants evaluated by Herbert et al.[22] and might be regarded as a "large" λ value, indicating that ice nucleation by cx-GNFs is relatively insensitive to changes in cooling rate.

The FROST analysis also reveals whether there is a strong particle-to-particle variability in ice nucleating ability. If the value d ln(n_s)/dT, termed ω, is equal to λ, then all surfaces of the nucleant have the same potential to nucleate ice. In contrast, if $\omega < \lambda$ then some parts of the surface have a greater potential to nucleate ice. For cx-GNFs cooled at 1 °C min^{-1} we have determined ω to be 0.83 °C^{-1}, which is clearly much smaller than λ. This suggests that the nucleation observed may be site specific, meaning that there may be specific sites on the cx-GNFs that are responsible for the ice nucleation.[21,22] The precise nature of these sites and the reason for their apparent nucleating activity is unclear. It is known that small molecules such as the water molecule can interact with carboxylic acid groups such as those present on cx-GNFs.[25−27] It may be that such site-specific interactions are related to the observed ice nucleation.

At present, there is no case where the mechanism of heterogeneous ice nucleation is well understood. Even the longstanding and elegant lattice matching hypothesis to which

the ice nucleating activity of silver iodide is attributed has been questioned.[28,29] Various molecular dynamics simulations have been conducted by a few different groups in order to address this issue.[30−35] This includes several studies looking specifically at carbon species.[36−39] Currently, there is a gap between experimental and computational work into ice nucleation that has proved very difficult to bridge, due to the vast differences in spatial scale and time scale of the systems that can be examined experimentally and computationally.

Recent work by Lupi et al.[38,39] using molecular dynamics simulations to study ice nucleation on carbon surfaces has provided certain qualitative predictions that it might be experimentally accessible. Specifically, they found that flat carbon surfaces without any oxidation or roughness nucleated ice most efficiently. Any oxidation,[38] roughness or curvature[39] was found to decrease the nucleation temperatures observed in the simulations. The result that oxidized carbon surfaces nucleate ice less well than pristine ones is somewhat counterintuitive and in contrast to the commonly stated "chemical bonding" requirement for ice nucleation,[3] as it might be expected that oxidation will offer greater opportunity for water to bond to a surface and so promote water structuring and ice nucleation. Our work here is consistent with the alternative hypothesis that a lower degree of oxidation leads to enhanced ice nucleation efficiency, although more species would need to be investigated to establish a statistically significant trend. Also, there are differences in structure and size between the nanomaterials investigated here, as well as extent of oxidation. These differences would need to be closely controlled to generate a firm experimental conclusion as to the effect of oxidation of carbon nanomaterials on ice nucleation efficiency. By thoroughly characterizing relatively simple ice nucleating species, it might be possible to conduct practical experiments that can be meaningfully related to computational studies. In general, by investigating closely related nucleants and observing differences in their ice nucleating efficiency, it may be possible to infer information about the causes of ice nucleating activity in these samples. Work here might be regarded as a first step in this direction and, now that their capacity to nucleate ice is known, carbon nanomaterials may prove to be a good candidate for further work on building a fundamental understanding of ice nucleation.

ASSOCIATED CONTENT

Supporting Information

Details of the synthesis of the carbon nanomaterials used, XPS analysis of the nanomaterials, the μL-NIPI ice nucleation instrument, and the FROST method for analysis of ice nucleation data are available in the Supporting Information. The Supporting Information is available free of charge on the ACS Publications website at DOI: 10.1021/acs.jpclett.5b01096.

AUTHOR INFORMATION

Corresponding Author

*E-mail: t.f.whale@leeds.ac.uk.

Notes

The authors declare no competing financial interest.

ACKNOWLEDGMENTS

REFERENCES

(1) Murray, B. J.; O'Sullivan, D.; Atkinson, J. D.; Webb, M. E. Ice Nucleation by Particles Immersed in Supercooled Cloud Droplets. *Chem. Soc. Rev.* **2012**, *41*, 6519−6554.

(2) Hoose, C.; Möhler, O. Heterogeneous Ice Nucleation on Atmospheric Aerosols: a Review of Results From Laboratory Experiments. *Atmos. Chem. Phys.* **2012**, *12*, 9817−9854.

(3) Pruppacher, H. R.; Klett, J. D. *Microphysics of Clouds and Precipitation*, 2nd ed.; Kluwer Academic Publishers: Dordrecht, The Netherlands, 1997.

(4) Morris, G. J.; Acton, E. Controlled Ice Nucleation in Cryopreservation - a Review. *Cryobiology* **2013**, *66*, 85−92.

(5) Searles, J. A.; Carpenter, J. F.; Randolph, T. W. The Ice Nucleation Temperature Determines the Primary Drying Rate of Lyophilization for Samples Frozen on a Temperature-Controlled Shelf. *J. Pharm. Sci.* **2001**, *90*, 860−871.

(6) Aksan, A.; Ragoonanan, V.; Hirschmugl, C. Freezing- and Drying-Induced Micro- and Nano-Heterogeneity in Biological Solutions. In *Biophysical Methods for Biotherapeutics*; John Wiley & Sons, Inc.: Hoboken, NJ, 2014.

(7) Kiani, H.; Sun, D. W. Water Crystallization and its Importance to Freezing of Foods: A Review. *Trends Food Sci. Technol.* **2011**, *22*, 407−426.

(8) Diehl, K.; Mitra, S. K. A Laboratory Study of the Effects of a Kerosene-Burner Exhaust on Ice Nucleation and the Evaporation Rate of Ice Crystals. *Atmos. Environ.* **1998**, *32*, 3145−3151.

(9) Demott, P. J. An Exploratory-Study of Ice Nucleation by Soot Aerosols. *J. Appl. Meteorol.* **1990**, *29*, 1072−1079.

(10) DeMott, P. J.; Prenni, A. J.; Liu, X.; Kreidenweis, S. M.; Petters, M. D.; Twohy, C. H.; Richardson, M. S.; Eidhammer, T.; Rogers, D. C. Predicting Global Atmospheric Ice Nuclei Distributions and Their Impacts on Climate. *Proc. Natl. Acad. Sci. U. S. A.* **2010**, *107*, 11217−11222.

(11) Pummer, B. G.; Bauer, H.; Bernardi, J.; Bleicher, S.; Grothe, H. Suspendable Macromolecules are Responsible for Ice Nucleation Activity of Birch and Conifer Pollen. *Atmos. Chem. Phys.* **2012**, *12*, 2541−2550.

(12) Fröhlich-Nowoisky, J.; Hill, T. C. J.; Pummer, B. G.; Franc, G. D.; Pöschl, U. Ice Nucleation Activity in the Widespread Soil Fungus Mortierella alpina. *Biogeosciences Discuss.* **2014**, *11*, 12697−12731.

(13) O'Sullivan, D.; Murray, B. J.; Ross, J. F.; Whale, T. F.; Price, H. C.; Atkinson, J. D.; Umo, N. S.; Webb, M. E. The Relevance of Nanoscale Biological Fragments for Ice Nucleation in Clouds. *Sci. Rep.* **2015**, *5*, 8082.

(14) Ogawa, S.; Koga, M.; Osanai, S. Anomalous Ice Nucleation Behavior in Aqueous Polyvinyl Alcohol Solutions. *Chem. Phys. Lett.* **2009**, *480*, 86−89.

(15) Salzmann, C. G.; Nicolosi, V.; Green, M. L. Edge-carboxylated Graphene Nanoflakes from Nitric Acid Oxidised Arc-discharge Material. *J. Mater. Chem.* **2010**, *20*, 314−319.

(16) He, H.; Riedl, T.; Lerf, A.; Klinowski, J. Solid-State NMR Studies of the Structure of Graphite Oxide. *J. Phys. Chem.* **1996**, *100*, 19954−19958.

(17) Whale, T. F.; Murray, B. J.; O'Sullivan, D.; Wilson, T. W.; Umo, N. S.; Baustian, K. J.; Atkinson, J. D.; Workneh, D. A.; Morris, G. J. A Technique for Quantifying Heterogeneous Ice Nucleation in Micro-litre Supercooled Water Droplets. *Atmos. Meas. Tech.* **2015**, *8*, 2437−2447.

(18) Umo, N. S.; Murray, B. J.; Baeza-Romero, M. T.; Jones, J. M.; Lea-Langton, A. R.; Malkin, T. L.; O'Sullivan, D.; Neve, L.; Plane, J. M.

C.; Williams, A. Ice Nucleation by Combustion Ash Particles at Conditions Relevant to Mixed-phase Clouds. *Atmos. Chem. Phys.* **2015**, *15*, 5195−5210.

(19) Riechers, B.; Wittbracht, F.; Hütten, A.; Koop, T. The Homogeneous Ice Nucleation Rate of Water Droplets Produced in a Microfluidic Device and the Role of Temperature Uncertainty. *Phys. Chem. Chem. Phys.* **2013**, *15*, 5873−5887.

(20) Murray, B. J.; Broadley, S. L.; Wilson, T. W.; Bull, S. J.; Wills, R. H.; Christenson, H. K.; Murray, E. J. Kinetics of the Homogeneous Freezing of Water. *Phys. Chem. Chem. Phys.* **2010**, *12*, 10380−7.

(21) Vali, G. Interpretation of Freezing Nucleation Experiments: Singular and Stochastic; Sites and Surfaces. *Atmos. Chem. Phys.* **2014**, *14*, 5271−5294.

(22) Herbert, R. J.; Murray, B. J.; Whale, T. F.; Dobbie, S. J.; Atkinson, J. D. Representing Time-Dependent Freezing Behaviour in Immersion Mode Ice Nucleation. *Atmos. Chem. Phys.* **2014**, *14*, 8501−8520.

(23) Koga, K.; Gao, G. T.; Tanaka, H.; Zeng, X. C. Formation of Ordered Ice Nanotubes Inside Carbon Nanotubes. *Nature* **2001**, *412*, 802−805.

(24) Pummer, B. G.; Budke, C.; Augustin-Bauditz, S.; Niedermeier, D.; Felgitsch, L.; Kampf, C. J.; Huber, R. G.; Liedl, K. R.; Loerting, T.; Moschen, T.; Schauperl, M.; et al. Ice Nucleation by Water-Soluble Macromolecules. *Atmos. Chem. Phys.* **2015**, *15*, 4077−4091.

(25) Cheng, J.; Soetjipto, C.; Hoffmann, M. R.; Colussi, A. J. Confocal Fluorescence Microscopy of the Morphology and Composition of Interstitial Fluids in Freezing Electrolyte Solutions. *J. Phys. Chem. Lett.* **2010**, *1*, 374−378.

(26) Guzmán, M. I.; Hildebrandt, L.; Colussi, A. J.; Hoffmann, M. R. Cooperative Hydration of Pyruvic Acid in Ice. *J. Am. Chem. Soc.* **2006**, *128*, 10621−10624.

(27) Guzmán, M. I.; Colussi, A. J.; Hoffmann, M. R. Photogeneration of Distant Radical Pairs in Aqueous Pyruvic Acid Glasses. *J. Phys. Chem. A* **2006**, *110*, 931−935.

(28) Finnegan, W. G.; Chai, S. K. A New Hypothesis for the Mechanism of ice Nucleation on Wetted AgI and AgI Center Dot AgCl Particulate Aerosols. *J. Atmos. Sci.* **2003**, *60*, 1723−1731.

(29) Massey, A.; McBride, F.; Darling, G. R.; Nakamura, M.; Hodgson, A. The Role of Lattice Parameter in Water Adsorption and Wetting of a Solid Surface. *Phys. Chem. Chem. Phys.* **2014**, *16*, 24018−24025.

(30) Hu, X. L.; Michaelides, A. Ice Formation on Kaolinite: Lattice Match or Amphoterism? *Surf. Sci.* **2007**, *601*, 5378−5381.

(31) Fraux, G.; Doye, J. P. K. Note: Heterogeneous Ice Nucleation on Silver-Iodide-Like Surfaces. *J. Chem. Phys.* **2014**, *141*, 216101.

(32) Reinhardt, A.; Doye, J. P. K. Effects of Surface Interactions on Heterogeneous Ice Nucleation for a Monatomic Water Model. *J. Chem. Phys.* **2014**, *141*, 084501.

(33) Cox, S. J.; Raza, Z.; Kathmann, S. M.; Slater, B.; Michaelides, A. The Microscopic Features of Heterogeneous Ice Nucleation May Affect the Macroscopic Morphology of Atmospheric Ice Crystals. *Faraday Discuss.* **2013**, *167*, 389−403.

(34) Cox, S. J.; Kathmann, S. M.; Purton, J. A.; Gillan, M. J.; Michaelides, A. Non-hexagonal Ice at Hexagonal Surfaces: the Role of Lattice Mismatch. *Phys. Chem. Chem. Phys.* **2012**, *14*, 7944−7949.

(35) Cox, S. J.; Kathmann, S. M.; Slater, B.; Michaelides, A. Molecular Simulations of Heterogeneous Ice Nucleation. I. Controlling Ice Nucleation Through Surface Hydrophilicity. *J. Chem. Phys.* **2015**, *142*, 184704.

(36) Cox, S. J.; Kathmann, S. M.; Slater, B.; Michaelides, A. Molecular Simulations of Heterogeneous Ice Nucleation. II. Peeling Back the Layers. *J. Chem. Phys.* **2015**, *142*, 184705.

(37) Cabriolu, R.; Li, T. Ice Nucleation on Carbon Surface Supports the Classical Theory for Heterogeneous Nucleation. *Phys. Rev. E: Stat. Phys., Plasmas, Fluids* **2015**, *91*, 052402.

(38) Lupi, L.; Molinero, V. Does Hydrophilicity of Carbon Particles Improve Their Ice Nucleation Ability? *J. Phys. Chem. A* **2014**, *118*, 7330−7337.

(39) Lupi, L.; Hudait, A.; Molinero, V. Heterogeneous Nucleation of Ice on Carbon Surfaces. *J. Am. Chem. Soc.* **2014**, *136*, 3156−3164.